



Published in final edited form as:

*Eur J Cell Biol.* 2009 December ; 88(12): 711–717. doi:10.1016/j.ejcb.2009.08.001.

## Golgi polarity does not correlate with speed or persistence of freely migrating fibroblasts

Andrea C. Uetrecht and James E. Bear\*

Lineberger Comprehensive Cancer Center and Department of Cell and Developmental Biology, University of North Carolina at Chapel Hill, 450 West Drive, CB#7295, 21-227 LCCC, Chapel Hill, 27599 NC, USA

### Abstract

The polarization of the Golgi has long been thought to be important for cell migration. Here we show that Rat2 cells at the edge of an artificial wound repolarize the Golgi relative to the nucleus to face the direction of migration into the wound. However, in the absence of cues from neighboring cells, individual cells do not display Golgi polarity relative to the direction in which they are moving. Instead, the positioning of the Golgi relative to the nucleus remains relatively constant over time and does not reflect changes in the direction of migration. Consistent with this observation, we observe only a slight bias in Golgi positioning to the front of the nucleus and this bias is not higher during periods of time when the cell is moving in a persistent manner. Taken together, these data suggest that Golgi polarity is not a requirement for cell migration.

### Keywords

Random migration; Wound healing; Scratch wound; Golgi morphology

### Introduction

Polarized cell migration is critical to many physiological processes including morphogenesis, immune response, and wound healing. One model for directional migration is the scratch-wound assay, in which a strip of cells is cleared from a confluent monolayer and the remaining cells migrate collectively to fill the gap. In this context, migration is accompanied by reorientation of the microtubule-organizing center (MTOC), centrosome and Golgi apparatus, relative to the nucleus, to face the direction of migration (DOM). In general, manipulations that interfere with reorientation of the MTOC/centrosome or the Golgi also block migration into the wound (Euteneuer and Schliwa, 1992; Gomes et al., 2005; Gotlieb et al., 1983). It has therefore been assumed that centrosome/Golgi polarization is a fundamental step in cell migration, although this has not been tested directly.

Whether this holds true for cells outside the context of the wound edge is unclear. Few studies have addressed the importance of MTOC/centrosome polarity for the migration of single cells. In freely migrating PtK2 cells the centrosome did not reorient when the cell changed direction (Danowski et al., 2001). In *Dictyostelium*, the formation of a pseudopod precedes centrosome

\*Corresponding author: Tel.: +1 919 966 5471; Fax: +1 919 966 3015; jbear@email.unc.edu (J.E. Bear).

**Publisher's Disclaimer:** This is a PDF file of an unedited manuscript that has been accepted for publication. As a service to our customers we are providing this early version of the manuscript. The manuscript will undergo copyediting, typesetting, and review of the resulting proof before it is published in its final citable form. Please note that during the production process errors may be discovered which could affect the content, and all legal disclaimers that apply to the journal pertain.

reorientation, and if this does not occur within 30 s, the pseudopod collapses (Ueda et al., 1997). These data suggest that centrosome positioning may be important for maintenance but not establishment of directed migration in freely migrating cells.

In this manuscript, we report for the first time the observation and analysis of Golgi position and morphology in live, freely migrating cells. Fluorescently tagged Golgi and nuclear markers were expressed in Rat2 fibroblasts and their positions were tracked in live cells. Contrary to the scratch-wound model, our data suggests that in freely migrating cells Golgi polarity is not a prerequisite for migration

## Materials and methods

### Materials

All materials were from Sigma unless otherwise indicated.

### Generation of polarity sensor cells

The polarity sensor vector was created in four basic steps. Primer sequences for all cloning steps are available on request. First, a bicistronic lenti-lox vector, pLL-5.5, was generated by replacing the GFP in pLL-5.0 (described by Cai et al., 2007) with the internal ribosomal entry sequence (IRES) from pQCXIX using standard PCR-based cloning techniques. Second, the Golgi-GFP marker was generated as follows. The sequence corresponding to the first 81 amino acids of human  $\beta$ -1,4-galactosyltransferase (GT) was PCR-amplified from human cDNA (first-strand reaction) and cloned into pML<sup>2</sup>-EGFP(N1) as an EcoRI/BamHI fragment by standard techniques. The GT-GFP fragment was subcloned into pLL-5.5 as an EcoRI/NotI (blunt) fragment upstream of the IRES to generate pLL-5.5-GIX. Third, the nuclear-mCherry marker was generated as follows. The Histone H2B (H2B)-encoding sequence was amplified from mouse cDNA and cloned into pML<sup>2</sup>-mCherry(N1) as a SacII/SalI fragment. The H2B-mCherry fragment was PCR-amplified and cloned into the blunted pLL-5.5 vector downstream of the IRES to generate pLL-5.5-XIH. To create the final vector, pLL-5.5-GIH, we made use of the two internal PciI sites in pLL-5.5 (one in the IRES, another in the vector backbone) by ligating together two PciI fragments from pLL-5.5-GIX and pLL-5.5-XIH containing either GT-GFP or H2B-mCherry, respectively. Lentiviral infections of Rat2 fibroblasts were carried out as previously described (Bear et al., 2002; Rubinson et al., 2003). Individual Rat2 cells infected with pLL-5.5-GIH were cloned by fluorescence-activated cell-sorting and screened for appropriate levels of expression.

### Cell culture and imaging conditions

Cells (ATCC) were maintained as previously described (Bear et al., 2002). For live-cell experiments, cells were adapted for several days to CO<sub>2</sub>-independent imaging medium: DME (Gibco) containing 4500 g/l glucose, 0.35 g/l NaHCO<sub>3</sub> and 25 mM HEPES, supplemented with 5% fetal bovine serum (FBS; Hyclone), 100 units/ml penicillin, 100  $\mu$ g/ml streptomycin and 292  $\mu$ g/ml glutamine. For live-cell scratch-wound assays, cells were plated on laminin (LN)-coated (50  $\mu$ g/ml) delta-T dishes (Bioptechs) at a density of  $4.2 \times 10^5$  cells/dish. The following day, the medium was replaced with serum-free medium containing 0.5% fatty acid-free BSA for 16–18 h prior to assays. Confluent monolayers were wounded using a 200- $\mu$ l pipet tip, washed two times with PBS and allowed to recover in imaging medium containing 5% FBS for 45 min prior to imaging. For single-cell migration, cells were adapted and plated as above but at a density of  $9.5 \times 10^3$  cells/dish and allowed to adhere overnight prior to imaging. For all live-cell imaging, media were supplemented with 6-hydroxy-2,5,7,8-tetramethylchroman-2-carboxylic acid (0.1 mM), ascorbate (0.5 mM) and catalase (10  $\mu$ g/ml).

## End-point assays and immunofluorescence

Cells were plated at the appropriate density on acid-washed LN-coated coverslips and allowed to adhere overnight. For nocodazole treatment, cells were pre-treated with 0.1  $\mu\text{g/ml}$  nocodazole for 1 h prior to wounding. Scratch assays were performed as above, and allowed to recover for 4 h in serum-containing media (with or without nocodazole) prior to fixation. Cells were fixed as described (Cai et al., 2007) and stained with Hoechst (1:10,000, Invitrogen), anti-GM130 (1:500, BD Transduction Laboratories) and anti-pericentrin (methanol fixation; 1:500, Covance) using standard techniques.

## Image acquisition and analysis

Images were captured in Slidebook (Olympus) using an IX-81 Olympus inverted microscope with a 20 $\times$  0.75NA dry objective, a CCD camera (C4742-80-12AG, Hamamatsu) and an automated X–Y stage. Images were exported as tiff files and analyzed using ImageJ. X–Y coordinates were exported to Excel (Microsoft) for calculations and graphing. Rose plots were generated in Aabel (Gigawiz, Ltd.) and statistical analysis was done in PRISM (Graph Pad, Inc.)

## Results and Discussion

### Polarity sensor validation

To assess whether Golgi polarity is related to migratory parameters, we developed a method to track the position of the Golgi apparatus relative to the nucleus in live cells over time. We designed a ‘polarity sensor’ to express fluorescent markers of both the nucleus (H2B-mCherry) and Golgi (GT-EGFP) (Fig. 1A). In Rat2 cells expressing this construct, GT-GFP co-localizes with the Golgi marker GM130 and H2B-mCherry co-localizes with Hoechst staining (Fig. S1). In addition, the Golgi marker co-localized with the centrosome marker pericentrin >80% of the time in sparsely plated cells (data not shown). To confirm that polarity sensor expression did not affect polarization, we performed end-point scratch-wound assays and assessed Golgi polarity after 4 h (Fig. 1B, C). Cells were considered polarized if the centroid of the Golgi was within  $\pm 60^\circ$  of the front of the nucleus (white lines, Fig. 1B). We observed no significant difference in Golgi polarization between control cells and polarity sensor cells (77% vs. 71%, respectively,  $p > 0.05$ , Fig. 1C). Previous studies demonstrated that MTOC and presumably Golgi polarity requires intact microtubules, and that low levels of nocodazole decreased MTOC reorientation (Euteneuer and Schliwa, 1992; Etienne-Manneville and Hall, 2001). We observed a similar decrease in Golgi polarization in both cell lines when treated with low levels of nocodazole (50% vs. 51%,  $p > 0.05$ , Fig. 1C).

### Heterogeneous Golgi morphology in sparsely plated cells

Polarity sensor cells plated under low-density conditions for single-cell migration assays display a more heterogeneous morphology than cells in the scratch-wound assay. We observed 7 categories of Golgi morphology (Fig. 1D) and quantified the relative abundance of each type under different plating conditions (Fig. 1E). For two categories, no clear Golgi centroid could be determined and these cells were excluded from analysis.

### The Golgi reorients to face the wound edge in a live-cell scratch-wound assay

Polarity sensor cells were observed live in a scratch-wound assay using time-lapse microscopy (Fig. 2A and Movie 1). Nuclear and Golgi positions were tracked by hand, as were cell positions because cell borders could not be unambiguously determined. From these three tracks, we calculated the Nuclear-Golgi axis (NGA) and the current DOM at every time-point (Fig. 2B). We plotted the angles of the current DOM and NGA vectors over time. As expected, the NGA is initially random relative to the long-term DOM, but over time the Golgi becomes oriented

to face into the wound. This trend was evident when we calculated the average absolute value of the NGA ( $|NGA|$ ) for the population over time (Fig. 2D). We also noticed that the current DOM fluctuated substantially despite the fact that this type of behavior was not evident in the time-lapse images. This likely reflects the fact that cells are moving slowly ( $<5$  pixels per frame or  $<0.3$   $\mu\text{m}/\text{min}$ ), and slight inaccuracies in tracking could result in significant fluctuations in the calculated current DOM (addressed below).

### Freely migrating cells have rapid changes in direction despite constant nucleus-Golgi positioning

We next examined Golgi positioning in sparsely plated, freely migrating cells (Fig. 2E and Movie 2). Cells underwent highly saltatory movement, characterized by periods of directionally persistent migration interspersed with periods of non-motility, or pauses, often associated with changes in direction. To minimize tracking inaccuracies revealed by our scratch-wound experiments (further investigated in Fig. S2), we outlined cells in every frame and determined the mathematical centroid of the cell to generate more accurate cell tracks. We plotted the current DOM and the NGA over time (Figs. 2F and S3A).

We were surprised to find that the NGA did not appear to align with either the current or long-term DOM. Rather Golgi positioning relative to the nucleus remains fairly constant over time, suggesting Golgi positioning is independent of the DOM in freely migrating cells. Changes in NGA are relatively slow, similar to a processing gyroscope. This ‘gyroscope-like’ behavior suggests that cells have the ability to maintain internal organization independent of peripheral structures such as the leading edge.

To investigate Golgi positioning during migration in a more quantitative way, we developed a metric ( $\theta$ ) of the relationship between the NGA and either the current DOM ( $\theta_C$ ) or the long-term DOM ( $\theta_{LT}$ ) (Fig. 3A). In either instance, a lower  $\theta$  indicates that the NGA is more aligned with the specified DOM. For the scratch-wound assay, we used  $\theta_{LT}$  since cells in this context were moving too slowly to accurately determine  $\theta_C$ , but maintained constant direction for the duration of the assay. During wound closure, the Golgi was distributed within  $\pm 60^\circ$  of the front of the nucleus 68.5% of the time (Fig. 3B). This result is in general agreement with results from traditional end-point scratch-wound assays (Fig. 1C).

The frequent directional changes (Movie 2) of freely migrating cells necessitated use of  $\theta_C$ . Therefore, we calculated  $\theta_C$  using either the accurate tracks from 10 outlined cells, or a larger cohort of hand-tracked cells that were filtered to eliminate all instances when the cell was moving too slowly to track accurately (Fig. S2B), and found that the Golgi was located in front of the nucleus approximately 45% of the time using either tracking method (Fig. 3B). Together, these data indicate that freely migrating cells have less polarized Golgi than cells migrating into a wound.

### Golgi polarity is not correlated with cell speed or persistence

We examined the relationship between speed and  $\theta_C$  for freely migrating cells (Fig. 3C). In general, we see no correlation between cell speed and Golgi polarity. Since freely migrating fibroblasts are saltatory, we developed a new metric to monitor persistence over short periods by modifying a standard directionality measurement,  $D/T$ , which is normally calculated over the course of an entire experiment. Instead, we calculated  $D/T$  in a sliding window over 20 min, which we called  $\text{RunD}/T$  (Fig. 3D). We examined the relationships between  $\theta_C$  and  $\text{RunD}/T$  over the course of a typical experiment (Figs. 3E, S3B) and observed no obvious relationship between these parameters (compare 120–180 min to 210–270 min, Fig. 3E). To generalize this observation across multiple cells, we compared the fraction of time when a cell had an oriented Golgi (ie.  $\theta_C$  between  $\pm 60^\circ$ ) across three categories of  $\text{RunD}/T$  and found that Golgi

polarization was equivalent (Fig. 3F). This indicates that Golgi polarization is not correlated with speed or directional persistence in freely migrating cells.

Cells at the wound edge polarize the Golgi to face the direction of migration, yet freely migrating cells do not. Several factors present in the wound edge environment may account for this. First, cells at the wound edge can form junctional complexes with neighboring cells on all sides except the one facing into the wound. Recent evidence has demonstrated the importance of cadherins in regulating MTOC/Golgi polarity at the wound edge (De Wever et al., 2004; Desai et al., 2009; Dupin et al., 2009). Freely migrating cells lack junctional input, which results in an uncoupling of Golgi-nuclear positioning from peripheral events. Second, it has been shown that single cells will adopt specific orientation of the centrosome, Golgi and nucleus, without migrating, when plated on geometrically constrained substrates (Thery et al., 2006), suggesting that geometrical constraints can also impinge on Golgi polarity. The wound edge may provide the spatial and signaling cues that can drive MTOC/Golgi polarity – cues that are absent during single cell migration. The factor(s) responsible for determining the direction of migration in freely migrating cells have yet to be fully elucidated.

## Supplementary Material

Refer to Web version on PubMed Central for supplementary material.

## Acknowledgments

We would like to thank Aaron Bradford for help with data processing and Sreeja Asokan, Bob Goldstein, Sarah Creed, Thomas Marshall, David Roadcap, and Tricia Wright for critical reading of the manuscript. This work was supported by grants from NIH (NCI, U54CA119343, GM083035)

## Abbreviations

<b>DOM</b>	Direction of migration
<b>EGFP</b>	Enhanced green fluorescent protein
<b>GT</b>	$\beta$ -1,4-Galactosyltransferase
<b>H2B</b>	Histone H2B
<b>LN</b>	Laminin
<b>MTOC</b>	Microtubule-organizing center
<b>NGA</b>	Nuclear-Golgi axis

## References

Bear JE, Svitkina TM, Krause M, Schafer DA, Loureiro JJ, Strasser GA, Maly IV, Chaga OY, Cooper JA, Borisy GG, Gertler FB. Antagonism between Ena/VASP proteins and actin filament capping regulates fibroblast motility. *Cell* 2002;109:509–521. [PubMed: 12086607]

- Cai L, Marshall TW, Utrecht AC, Schafer DA, Bear JE. Coronin 1B coordinates Arp2/3 complex and cofilin activities at the leading edge. *Cell* 2007;128:915–929. [PubMed: 17350576]
- Danowski BA, Khodjakov A, Wadsworth P. Centrosome behavior in motile HGF-treated PtK2 cells expressing GFP-gamma tubulin. *Cell Motil Cytoskeleton* 2001;50:59–68. [PubMed: 11746672]
- De Wever O, Westbroek W, Verloes A, Bloemen N, Bracke M, Gespach C, Bruyneel E, Mareel M. Critical role of N-cadherin in myofibroblast invasion and migration in vitro stimulated by colon-cancer-cell-derived TGF-beta or wounding. *J Cell Sci* 2004;117:4691–4703. [PubMed: 15331629]
- Desai RA, Gao L, Raghavan S, Liu WF, Chen CS. Cell polarity triggered by cell-cell adhesion via E-cadherin. *J Cell Sci* 2009;122:905–911. [PubMed: 19258396]
- Dupin I, Camand E, Etienne-Manneville S. Classical cadherins control nucleus and centrosome position and cell polarity. *J Cell Biol* 2009;185:779–786. [PubMed: 19487453]
- Etienne-Manneville S, Hall A. Integrin-mediated activation of Cdc42 controls cell polarity in migrating astrocytes through PKCzeta. *Cell* 2001;106:489–498. [PubMed: 11525734]
- Euteneuer U, Schliwa M. Mechanism of centrosome positioning during the wound response in BSC-1 cells. *J Cell Biol* 1992;116:1157–1166. [PubMed: 1740470]
- Gomes ER, Jani S, Gundersen GG. Nuclear movement regulated by Cdc42, MRCK, myosin, and actin flow establishes MTOC polarization in migrating cells. *Cell* 2005;121:451–463. [PubMed: 15882626]
- Gotlieb AI, Subrahmanyam L, Kalnins VI. Microtubule-organizing centers and cell migration: effect of inhibition of migration and microtubule disruption in endothelial cells. *J Cell Biol* 1983;96:1266–1272. [PubMed: 6341378]
- Rubinson DA, Dillon CP, Kwiatkowski AV, Sievers C, Yang L, Kopinja J, Rooney DL, Zhang M, Ihrig MM, McManus MT, Gertler FB, Scott ML, Van Parijs L. A lentivirus-based system to functionally silence genes in primary mammalian cells, stem cells and transgenic mice by RNA interference. *Nat Genet* 2003;33:401–406. [PubMed: 12590264]
- They M, Racine V, Piel M, Pepin A, Dimitrov A, Chen Y, Sibarita JB, Bornens M. Anisotropy of cell adhesive microenvironment governs cell internal organization and orientation of polarity. *Proc Natl Acad Sci USA* 2006;103:19771–19776. [PubMed: 17179050]
- Ueda M, Graf R, MacWilliams HK, Schliwa M, Euteneuer U. Centrosome positioning and directionality of cell movements. *Proc Natl Acad Sci USA* 1997;94:9674–9678. [PubMed: 9275182]

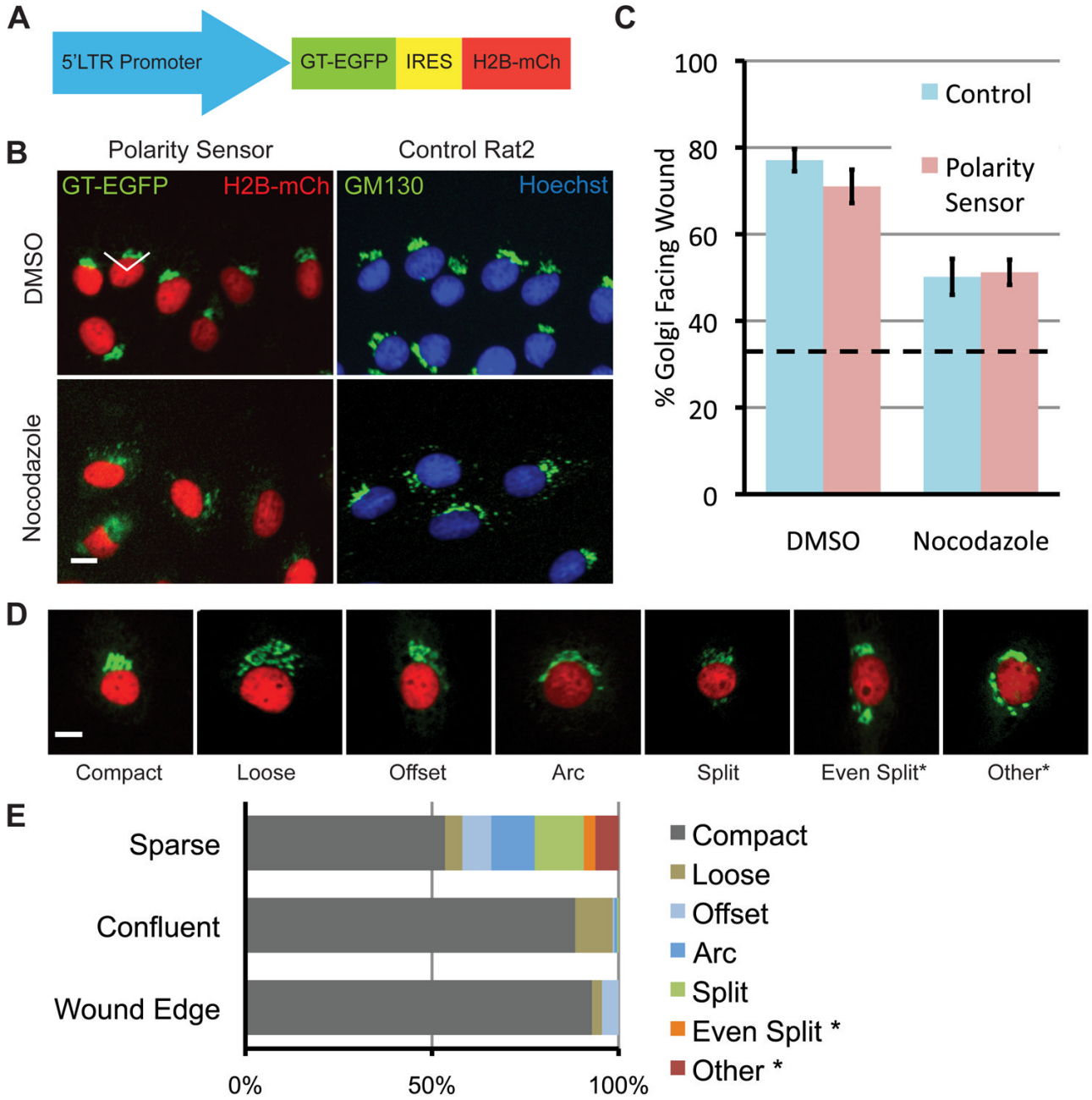


**Fig. 1.** Characterization of the polarity sensor. (A) Polarity sensor design. The Golgi is marked with the first 81 amino acids of GT fused to EGFP. The nucleus is marked with H2B fused to mCherry. These sequences flank an internal ribosomal entry sequence (IRES) to allow simultaneous expression from a single promoter. (B) Representative images of cells in the scratch-wound assay treated with either DMSO (control) or nocodazole (0.1  $\mu\text{g}/\text{ml}$ ). Uninfected Rat2 cells are labeled with anti-GM130 (green) and Hoechst (blue) to mark the Golgi and nucleus, respectively. The wound edge is up, the white lines indicate  $\pm 60^\circ$  facing the wound edge, considered polarized. Scale bar = 10  $\mu\text{m}$ . (C) Quantification of results in (B). Results are from at least 100 cells per treatment from each of 3 independent experiments. Data

were analyzed using one-way ANOVA and Tukey's post-hoc test. Error bars = S.E.M.; dashed line indicates random Golgi positioning. (D) Golgi morphology is heterogeneous. Representative images of different Golgi morphologies observed in sparsely plated cells. Scale bar = 10  $\mu\text{m}$ . (E) Quantification of results in (D). Two categories of Golgi morphology, indicated by asterisks, were excluded from subsequent analyses because the Golgi position could not be determined.



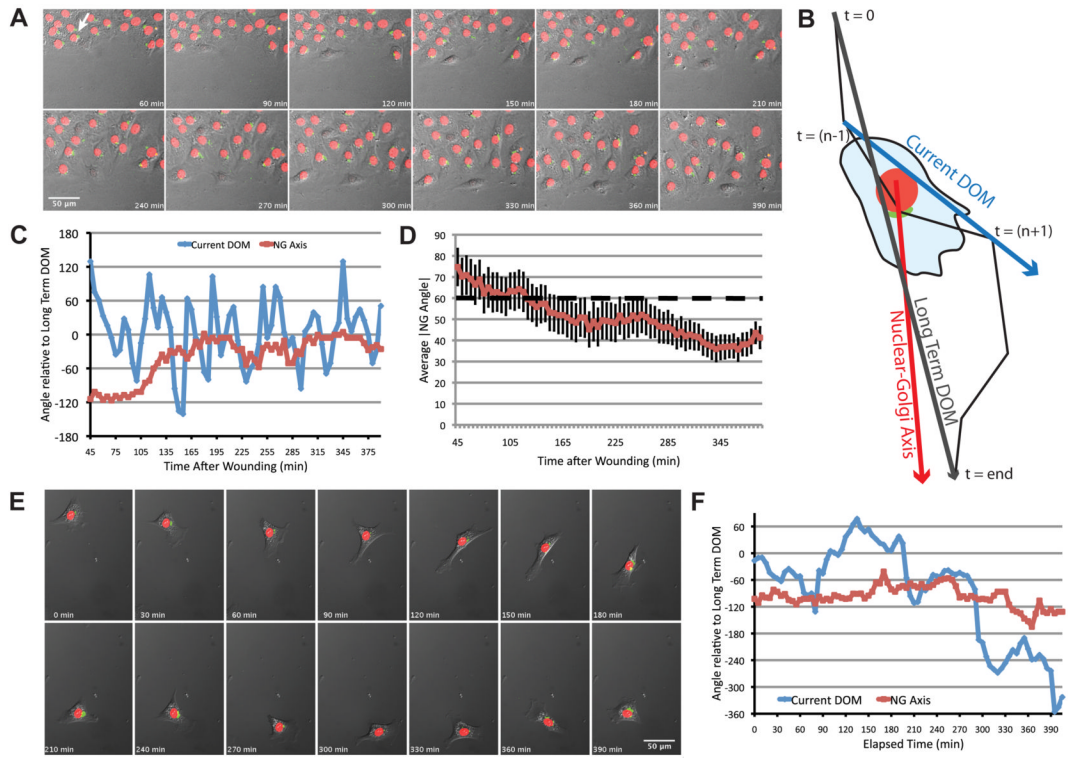


**Fig. 2.**

The NGA aligns with the direction of migration into the wound but does not align with the direction of migration in freely migrating cells. (A) Representative time-lapse images of Rat2 cells expressing the polarity sensor in the scratch-wound assay. The arrow indicates the cell analyzed in (C). (B) Schematic diagram of axes used for analysis. The cell track is represented by the black line, from  $t=0$  to  $t=end$ . These two points define the long-term DOM (turquoise arrow). The current DOM at  $t=n$  is defined by the position of the cell centroid at  $t=(n-1)$  and  $t=(n+1)$  (blue arrow). The NGA is the vector defined by the current nuclear and Golgi positions (red arrow). (C) Current DOM and NGA relative to the long-term DOM over time for the representative cell indicated in (A). (D) The average absolute value of NGA relative to the long-term DOM for multiple cells ( $n\sim 60$ ) in the wound healing assay over time. Error bars = S.e.M. (E) Time-lapse images of a freely migrating cell expressing the polarity sensor. (F) Current DOM and NGA of the cell in (E) relative to the long-term DOM over time. In this case, DOM was calculated from the hand-outlined track.

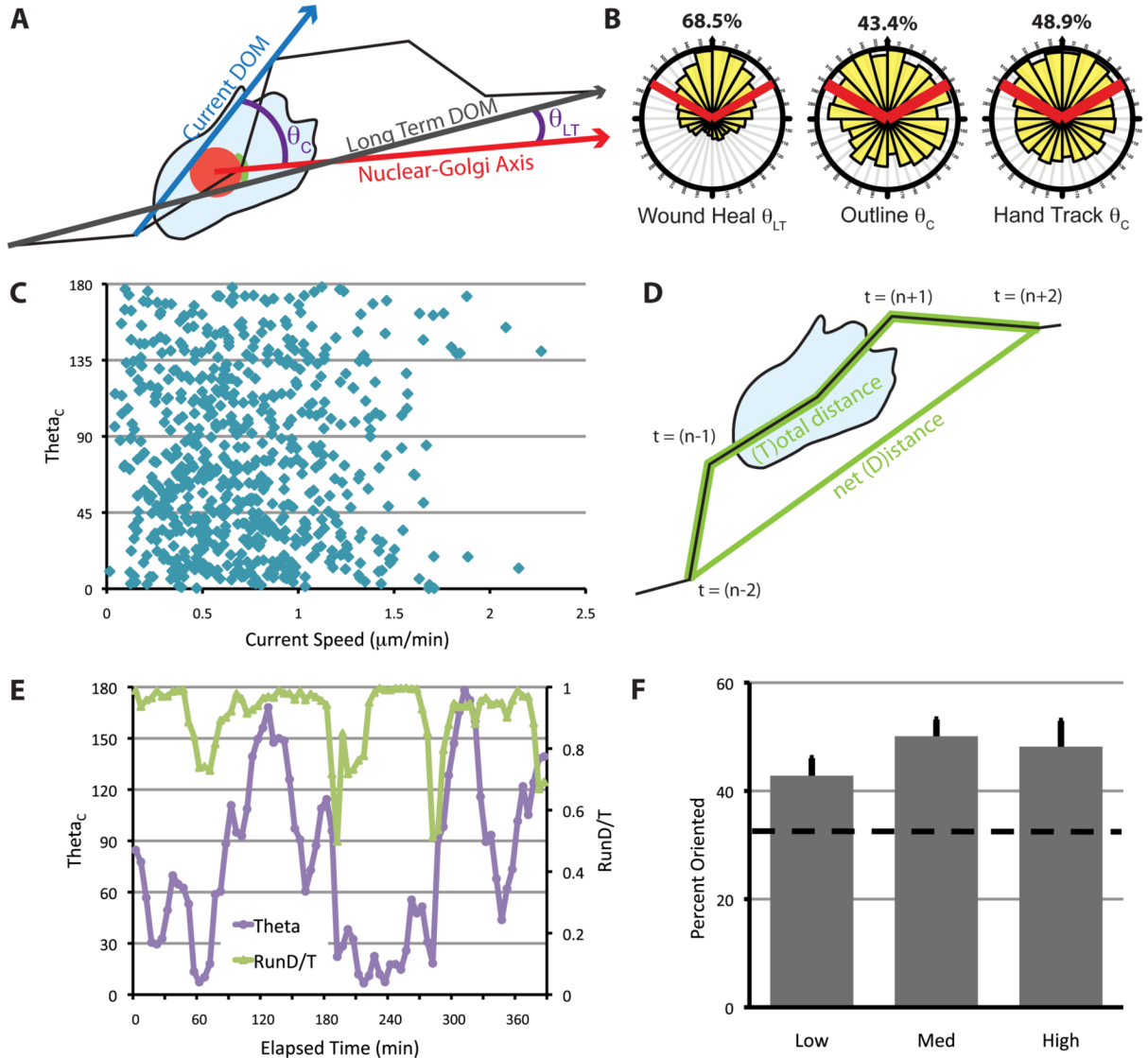


**Fig. 3.** Nucleus-Golgi polarity is not correlated with the direction of migration in freely migrating cells. (A) Schematic for calculating  $\theta$ .  $\theta_{LT}$  is used for cells in the scratch wound assay and  $\theta_C$  is used for freely migrating cells. The current DOM (and  $\theta_C$ ) was calculated from cell centroids determined in two ways, as described in the text and Fig. S1. (B) The distribution of  $\theta$  for cells at the wound edge or in freely migrating cells. Red lines indicate  $\pm 60^\circ$  facing the DOM, and the percentage of data that fall within these boundaries are indicated above. Data were generated from at least three independent experiments with at least 100 cells total for each condition, tracked over at least 5 h. (C)  $\theta$  as a function of current cell speed. Current cell speed was calculated using tracks from outlined cells over 10 min from  $(t-1)$  to  $(t+1)$ . (D)  $RunD/T$  was calculated as a sliding window using cell centroids from time  $(t-2)$ ,  $(t-1)$ ,  $(t)$ ,  $(t+1)$  and  $(t+2)$ .  $D/T$  is defined as the net path length ( $D$ ) divided by the total path length ( $T$ ). (E)  $\theta$  and  $RunD/T$  for the cell shown in Fig. 2E over time.  $RunD/T$  was calculated from the hand-outlined track of this cell. (F) Percentage of times when the Golgi is oriented ( $\theta < 60^\circ$ ), during times when  $RunD/T$  is high ( $\geq 0.9$ ), medium ( $0.9 > RunD/T > 0.7$ ) or low ( $< 0.7$ ) in freely migrating cells.  $RunD/T$  was calculated from the hand-tracked positions, and instances

when cells were deemed too slow for accurate tracking were eliminated (see Fig. S1). The dashed line indicates random Golgi positioning. Error bars = S.E.M. Data were generated from four independent experiments with at least 100 cells total.